

# Complex-Time (Kime) Representation of Spatiotemporal Processes and Spacekime Analytics

Kime-Phase Tomography (KPT)

---

Ivo D. Dinov, Yueyang Shen & Bojko Bakalov

March 8, 2026

SOCR · University of Michigan · North Carolina State University

<https://SOCR.umich.edu> | <https://TCIU.predictive.space/>



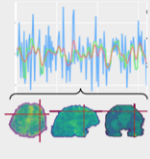
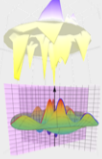
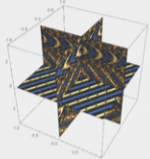
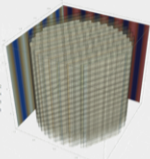
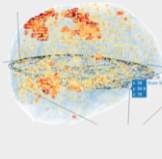
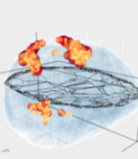
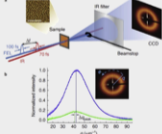
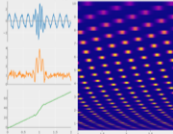
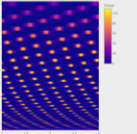
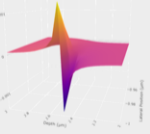
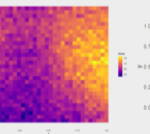

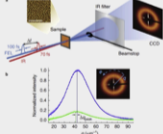
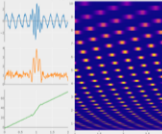
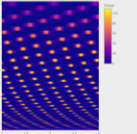
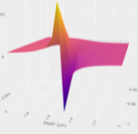
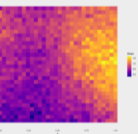

1. Motivation and Problem Setting
2. Mathematical Foundations
3. Inference and Space-Time Analytics
4. Applications and Validation (Simulations)
5. Limitations and Opportunities
6. Summary

Kime-Surface Representation

# 1. Motivation and Problem Setting

---

# Idea: Longitudinal Data $\rightarrow$ Kime-Transforms $\rightarrow$ PDEs $\rightarrow$ AI/ML

Apps	Time $\rightarrow$ Kime Transformation	Wave equation Solutions (kime) dynamics			Prospective Data Science Applications																				
<b>Biomed</b>							fMRI time-series	fMRI kime-surfaces	Cross sections	Volume rendering	3D p-value map	Stat significance	<b>Physics</b>							Time-dynamic structural phase transitions	Wavelet or Hilbert transform of time-dependent diffraction	Takagi-Taupin PDE model of dynamical X-ray diffraction in deformed crystals	Phonon modes at phase transition		
	fMRI time-series	fMRI kime-surfaces	Cross sections	Volume rendering	3D p-value map	Stat significance																			
<b>Physics</b>							Time-dynamic structural phase transitions	Wavelet or Hilbert transform of time-dependent diffraction	Takagi-Taupin PDE model of dynamical X-ray diffraction in deformed crystals	Phonon modes at phase transition															
	Time-dynamic structural phase transitions	Wavelet or Hilbert transform of time-dependent diffraction	Takagi-Taupin PDE model of dynamical X-ray diffraction in deformed crystals	Phonon modes at phase transition																					

## Why kime? Why tomography?

- **Observed problem:** repeated measurements at the same chronological time often exhibit large *structured* variability (not just additive noise).
- **Consequence:** averaging/denoising can erase latent state structure, leading to miscalibrated inference or degraded prediction.
- **KPT goal:** decompose replicate variability into

extrinsic (range-space) noise + intrinsic (domain-space) phase variability.

- **Kime representation:** augment time  $t$  by a latent phase  $\theta \in \mathbb{S}^1$ , forming a complex-time coordinate

$$\kappa = t e^{i\theta} \in \mathbb{C},$$

enabling *phase-resolved* inference and prediction.

## Rationale for Time $\longrightarrow$ Kime Extension

- **Math:** *Time* is a special case of *Kime*,  $\kappa = t e^{i\theta} \in \mathbb{C}$ , where  $\theta = 0$ . Time ( $\mathbb{R}^+$ ) is a subgroup of the multiplicative Reals group. Whereas kime ( $\mathbb{C}$ ) is an algebraically closed field that naturally extends time. Time is ordered, kime is not! As a complete field, *Kime* represents the smallest natural extension of *Time*.
- **Physics:**
  - The *Problem of Time*: Time has different meanings in quantum mechanics & general relativity; leading to a tension in formulating a Quantum Gravity Theory unifying the two (DOI 10.1007/978-3-319-58848-3).
  - (Base-field)  $\mathbb{R}$  and  $\mathbb{C}$  based Hilbert-space quantum theories make different predictions (DOI: 10.1038/s41586-021-04160-4).
- *AI/Data Science*: Random IID sampling, Bayesian representations, tensor modeling of  $\mathbb{C}$  kimesurfaces & novel analytics.

Wesson (2010); Dinov & Velev (2021); Wang et al. (2022); Zhang et al. (2023); Dinov & Shen (2024).

# KPT data model (replicated longitudinal processes)

For time points  $t_k \in (0, T]$  and replicates  $j = 1, \dots, N$ :

$$\underbrace{\Theta_{j,k}}_{\text{stochastic phase}} \sim \underbrace{\varphi_{t_k}(\theta)}_{\text{latent phase law on } \mathbb{S}^1}$$
$$\underbrace{y_{j,k} \mid \Theta_{j,k}}_{\text{observed measurements}} \sim p(y \mid \theta; t_k, \mathcal{S})$$

A common likelihood (used in simulations and algorithms):

$$y_{j,k} = \mathcal{S}(t_k, \Theta_{j,k}) + \varepsilon_{j,k}, \quad \varepsilon_{j,k} \sim \mathcal{N}(0, \sigma^2).$$

Model Kime-Surface

**Unknown objects:**

kime-surface  $\mathcal{S}(t, \theta)$  and phase density  $\varphi_t(\theta) \in \mathcal{P}$ .

# Problem Solved by Kime-Phase Tomography (KPT)

## KPT capability

Given replicated longitudinal observations  $\{y_{j,k}\}$ , KPT reconstructs a coupled pair

$$(\widehat{S}(t, \theta), \widehat{\varphi}_t(\theta))$$

that explains structured replicate-to-replicate variability as a time-evolving phase distribution on  $\mathbb{S}^1$ .

- **Interpretability:**  $\widehat{\varphi}_t$  quantifies latent state concentration, drift, multimodality.
- **Prediction:** synthetic draws  $\theta \sim \widehat{\varphi}_t$  and evaluation of  $\widehat{S}(t, \theta)$  induce predictive distributions.
- **Scalability:** FFT-based spectral updates enable fast inference on dense time grids.

## 2. Mathematical Foundations

---

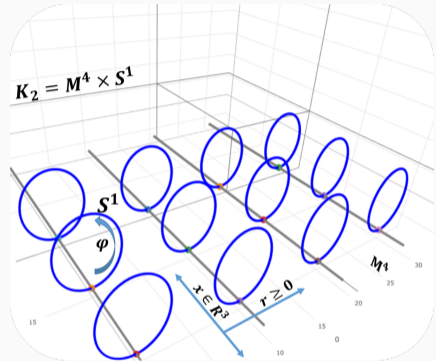
# Historical Background: Kaluza-Klein Theory

Theodor Kaluza (1921) developed a *math extension of the classical general relativity theory to 5D*. This included the metric, the field equations, the equations of motion, the stress-energy tensor, and the cylinder condition.

Physicist Oskar Klein (1926) *interpreted Kaluza's 3D+2D theory in quantum mechanical space* and proposed that the fifth dimension was curled up and microscopic.

The topology of the 5D Kaluza-Klein spacetime is  $\mathbb{K}_2 \simeq \mathbb{M} \times \mathbb{S}^1$ , where  $\mathbb{M}$  is a 4D Minkowski spacetime and  $\mathbb{S}^1$  is a circle (non-traversable).

(Kaluza) DOI: 10.1142/S0218271818700017; (Klein) DOI: 10.1007/BF01397481; (Bailin & Love) DOI 10.1088/0034-4885/50/9/001



# Ultrahyperbolic PDEs: Wave Equation – Cauchy Initial Data

For ultrahyperbolic PDEs, the (*unconstrained*) initial value problem, determining the solution(s) for a given initial condition, is *ill-posed*.

No guarantee of a global well-defined, stable, and unique solution!

Nonlocal constraints yield the existence, uniqueness & stability of local and global solutions to the *ultrahyperbolic wave equation* under Cauchy initial data.

Spacekime Wave Equ  
Sol

$$\underbrace{\sum_{i=1}^{d_s} \partial_{x_i}^2 u := \Delta_x u(x, \kappa)}_{\text{spacial Laplacian}} = \underbrace{\Delta_\kappa u(x, \kappa) := \sum_{i=1}^{d_t} \partial_{\kappa_i}^2 u}_{\text{temporal Laplacian}}, \left\{ \begin{array}{l} u_0 = u(x \in D_s; (0, \kappa_{-1}) \in D_t) \\ u_1 = \partial_{\kappa_1} u(x, (0, \kappa_{-1})) \end{array} \right\} \underbrace{\hspace{10em}}_{\text{initial conditions (Cauchy data)}}$$

$\exists$  stable local solution over a Fourier frequency region, nonlocal constraints,  $|\xi| \geq |\eta_{-1}|$ .

$$\hat{u}(\xi, \kappa_1, \eta_{-1}) = \cos(2\pi\kappa_1 \sqrt{|\xi|^2 - |\eta_{-1}|^2}) \hat{u}_0(\xi, \eta_{-1}) + \sin(2\pi\kappa_1 \sqrt{|\xi|^2 - |\eta_{-1}|^2}) \frac{\hat{u}_1(\xi, \eta_{-1})}{2\pi \sqrt{|\xi|^2 - |\eta_{-1}|^2}}.$$

## Kime manifold, metric, and cone measure

- Domain:  $\mathcal{M} = (0, T] \times \mathbb{S}^1$  with cone metric

$$g_0 = dt^2 + t^2 d\theta^2.$$

- Natural measure (cone measure):

$$d\mu_{g_0} = t dt \otimes \frac{d\theta}{2\pi}.$$

- Hilbert space:

$$\mathcal{H} = L^2(\mathcal{M}, d\mu_{g_0}).$$

### Remark

The geometry induces the correct inner products, Sobolev penalties, and spectral regularization aligned with polar coordinates.

## Laplace-Beltrami operator on the cone

On  $(\mathcal{M}, g_0)$ , the Laplace-Beltrami operator is

$$\Delta_{g_0} = \frac{1}{t} \frac{\partial}{\partial t} \left( t \frac{\partial}{\partial t} \right) + \frac{1}{t^2} \frac{\partial^2}{\partial \theta^2}.$$

- Used to motivate smoothness penalties and spectral bases.
- Eigenstructures connect to Bessel functions (regularity at  $t = 0$ , boundary at  $t = T$ ).
- Enables anisotropic regularization aligned with the cone geometry (future extensions).

# Harmonic expansions and kime-surface representation

Represent the kime-surface and phase law using harmonics in  $\theta$ :

$$\mathcal{S}(t, \theta) = \sum_{n \in \mathbb{Z}} f_n(t) e^{in\theta}, \quad f_{-n}(t) = \overline{f_n(t)},$$
$$\varphi_t(\theta) = \sum_{n \in \mathbb{Z}} \hat{\varphi}_t(n) e^{in\theta}, \quad \hat{\varphi}_t(0) = 1.$$

Truncation to  $n \in \{-J, \dots, J\}$  yields efficient computation and controlled bias.

## Mixed moments and posterior harmonics (KPT E-step objects)

For Gaussian likelihood  $Y | \theta \sim N(\mathcal{S}(t, \theta), \sigma^2)$ :

$$p(\theta | y; t) \propto \varphi_t(\theta) \exp\left(-\frac{(y - \mathcal{S}(t, \theta))^2}{2\sigma^2}\right).$$

Define posterior harmonic expectations

$$\xi_{j,k}(n) = \mathbb{E}\left[e^{-in\Theta_{j,k}} | y_{j,k}\right] = \int_0^{2\pi} e^{-in\theta} p(\theta | y_{j,k}; t_k) \frac{d\theta}{2\pi}.$$

Empirical mixed moments:

$$\hat{m}_n(t_k) = \frac{1}{N} \sum_{j=1}^N y_{j,k} \xi_{j,k}(n).$$

## Key spectral factorization: convolution $\rightarrow$ product

Define generating functions (or Fourier series on the unit circle):

$$\underbrace{M(z, t) = \sum_n m_n(t) z^n}_{FT(\text{mixed-moments})}, \quad \underbrace{F(z, t) = \sum_n f_n(t) z^n}_{FT(\text{kime-surface})}, \quad \underbrace{\Phi(z, t) = \sum_n \hat{\varphi}_t(n) z^n}_{FT(\text{phase}), \quad |z| = 1.}$$

**Core KPT identity (on  $|z| = 1$ )**

$$M(z, t) = F(z, t) \Phi(z, t).$$

- Mixed moments are a convolution in  $n$ , which becomes pointwise multiplication in the generating-function / DFT domain.
- Enables regularized deconvolution updates for  $\Phi$  and  $F$ .

## Gauge (rotation) ambiguity and anchoring

A joint circular shift  $\theta \mapsto \theta + \alpha(t)$  induces

$$\varphi_t(\theta) \mapsto \varphi_t(\theta - \alpha(t)), \quad \mathcal{S}(t, \theta) \mapsto \mathcal{S}(t, \theta - \alpha(t)),$$

leaving the composed signal distribution invariant.

- **Rotation-invariant functionals:**  $|\widehat{\varphi}_t(n)|$ , Sobolev energies, distances.
- **Directional functionals:** mean direction, V-tests, phase-aligned comparisons require anchoring.
- **Anchoring rule (example):** choose  $n_\star \geq 1$  with  $|\widehat{\varphi}_t(n_\star)| > 0$  and rotate so  $\widehat{\varphi}_t(n_\star)$  is real and  $> 0$ .

Three Longitudinal Processes  
over the *Kime manifold*.

### **3. Inference and Space-Time Analytics**

---

## Inference from KPT outputs

Given estimated phases,  $\hat{\varphi}_{t,estim}(\theta)$ , or their Fourier coefficients,  $\hat{\varphi}_{t,FT}(n)$ , we perform

- **Uniformity tests** (Rayleigh-type based on first harmonic magnitude).
- **Directional alternatives** (V-test; requires anchoring).
- **Two-sample comparisons** via weighted Fourier distances.
- **Across-time inference** with multiplicity control over  $\{t_k\}$ .
- **Uncertainty quantification** via spectral delta method and/or bootstrapping.

## Regularization-induced shrinkage and de-biasing

Let  $\Lambda_p(\omega) = (2 \sin(\frac{\omega}{2}))^{2p}$  be the discrete Sobolev weight of order  $p \in \{0, 1, 2\}$ . A Wiener-Sobolev update implies shrinkage factor

$$H(\omega, t) = \frac{|\widehat{F}(\omega, t)|^2}{|\widehat{F}(\omega, t)|^2 + \lambda_\Phi \Lambda_{p_\Phi}(\omega)} \in (0, 1].$$

De-biased spectrum (when stable):

$$\widetilde{\Phi}(\omega, t) = \frac{\widehat{\Phi}(\omega, t)}{H(\omega, t)} = \frac{\overline{\widehat{F}(\omega, t)}}{|\widehat{F}(\omega, t)|^2} \widehat{M}(\omega, t) \quad (\text{optionally with ridge}).$$

- Extract first harmonic (or other modes) from  $\widetilde{\Phi}$  for asymptotic calibration.
- If  $|\widehat{F}|$  is small, prefer bootstrap calibration.

## Space-time analytics (SKA): spatial extension

Let observations be indexed by spatial location  $s$  (voxel, pixel, sensor, region).

$$y_{j,k}(s) = \mathcal{S}(t_k, \Theta_{j,k}(s); s) + \varepsilon_{j,k}(s), \quad \Theta_{j,k}(s) \sim \varphi_{t_k}(\cdot; s).$$

- Estimate  $\hat{\varphi}_t(\theta; s)$  and  $\hat{\mathcal{S}}(t, \theta; s)$  across  $s$ .
- Spatial regularization on harmonic coefficients (optional).
- Outputs: maps of phase concentration, drift, multimodality; phase-conditioned response maps.

## **4. Applications and Validation (Simulations)**

---

## Validation protocol: two motivating case studies

- **Simulation Study I:** quantum double-slit experiment with run-to-run phase variability.
- **Simulation Study II:** synthetic event-related fMRI ON–OFF design with time-varying latent physiological state.
- Both demonstrate core tenet: *apparent noise* can be decomposed into extrinsic noise + intrinsic time-phase variability.

### Reproducibility

End-to-end computational protocol and figures are provided in the supplemental Rmd notebook / supporting website.

# Double-slit: qualitative reconstruction of kime-surface

- Recover  $\widehat{\mathcal{S}}(t, \theta)$  from repeated noisy observations.
- Compare true vs. KPT-GEM and KPT-FFT reconstructions.

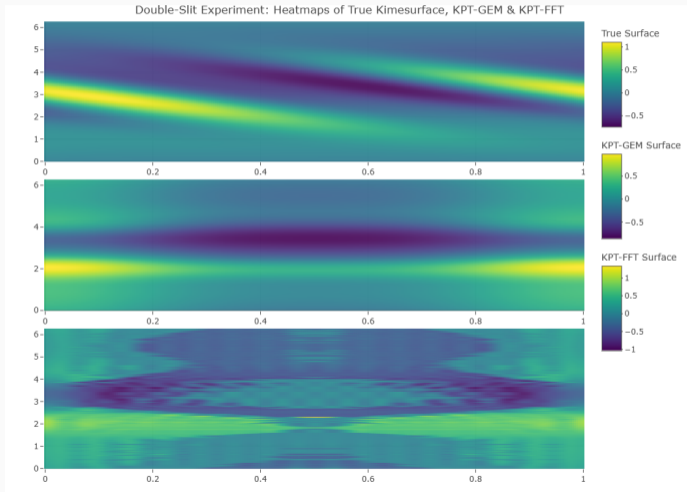


Figure: True vs. KPT reconstructions of  $\mathcal{S}(t, \theta)$ .

# Double-slit: phase recovery metrics across time

- Time-varying KL/JSD/Hellinger/TV between true  $\varphi_t$  and estimated  $\hat{\varphi}_t$ .

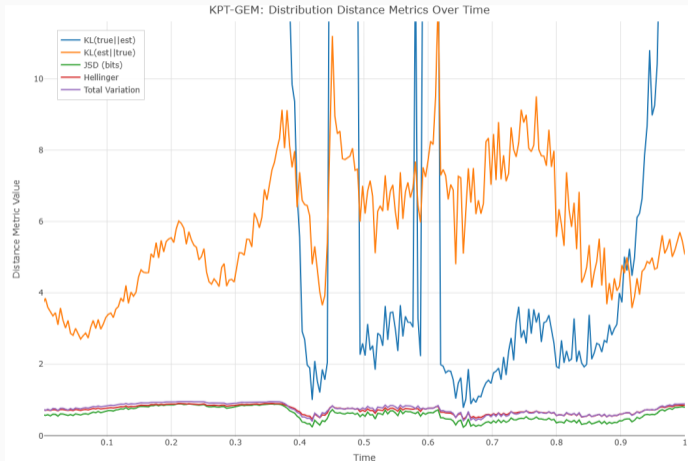
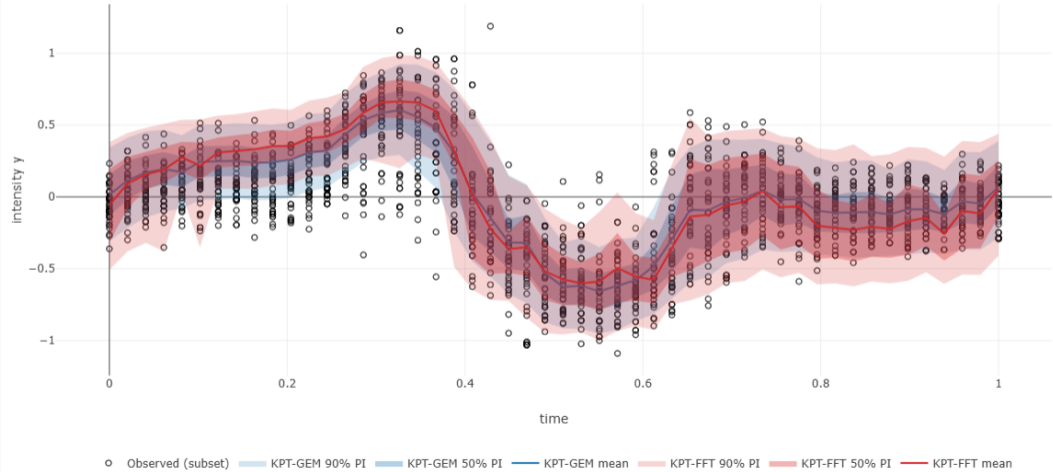


Figure: Phase metrics vs. time (KPT-GEM).

# Double-slit: predictive fit and confidence bands

Compare mean MAP curves and confidence bands to observed scatter.

Double-slit: Observations (open circles) vs. KPT predictive bands



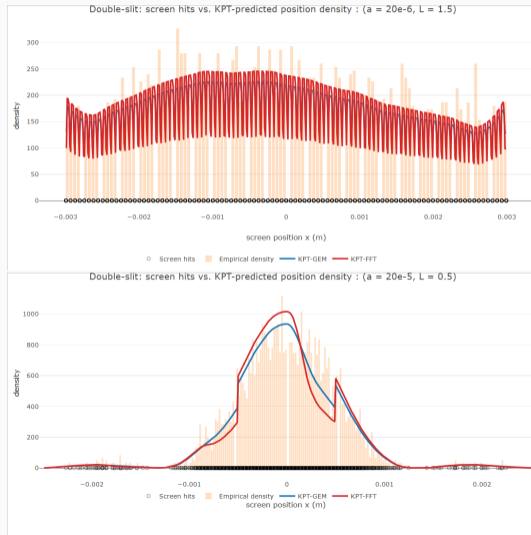
## Double-slit: summary metrics

**Table:** Double-Slit Experiment: Summary metrics comparing true kime-surface vs. KPT reconstructions (KPT-GEM, KPT-FFT).

Algorithm	Mean JSD (bits)	Mean Hellinger	Mean TV	Rel. L2 Surface
KPT-GEM	0.6072	0.7266	0.7532	1.2514
KPT-FFT	0.6101	0.7302	0.7524	1.5167

# Double-slit: posterior predictive position density (physics linkage)

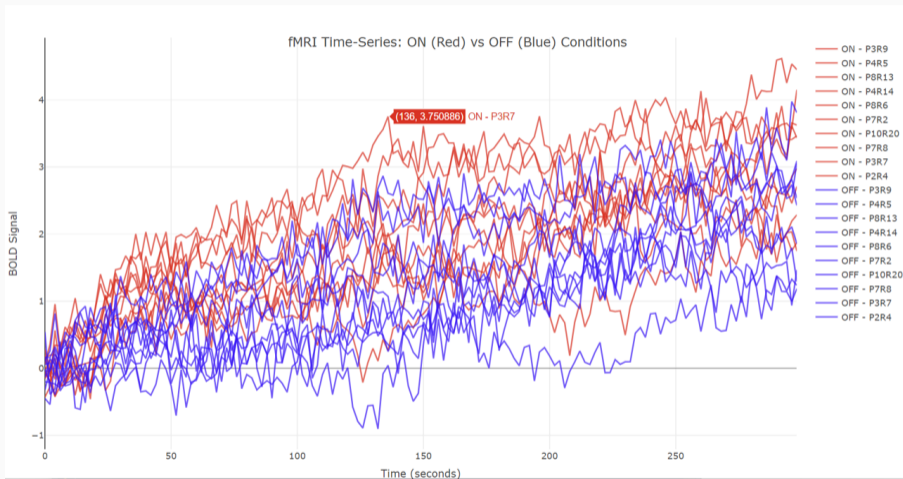
- Use recovered kime objects  $\{\widehat{S}(t, \theta), \widehat{\varphi}_t(\theta)\}$  to predict the screen-hit position distribution.
- Two different parameter sets: Observed hits vs. KPT predicted posterior density (two parameter settings).
- Interpretation: KPT transforms run-to-run interference fluctuations into an inferred phase law and a deterministic kime-surface.



## fMRI simulation: setup and motivation

- Simulate event-related ON vs. OFF fMRI design with repeated runs per participant.
- Input to KPT: difference signal  $y_{j,r,k} = \text{ON}_{j,r,k} - \text{OFF}_{j,r,k}$  to isolate task activation.
- KPT hypothesis: substantial run-to-run variability arises from intrinsic physiological state, modeled as latent time-phase  $\Theta(t)$ .

# fMRI: raw simulated trajectories



**Figure:** Examples of simulated ON and OFF fMRI time-courses for random participants (P) and runs (R).

# fMRI: phase recovery metrics vs. time (JSD bits)

Symmetric Jensen-Shannon divergence (bits) across time between true & estimated  $\varphi_t$

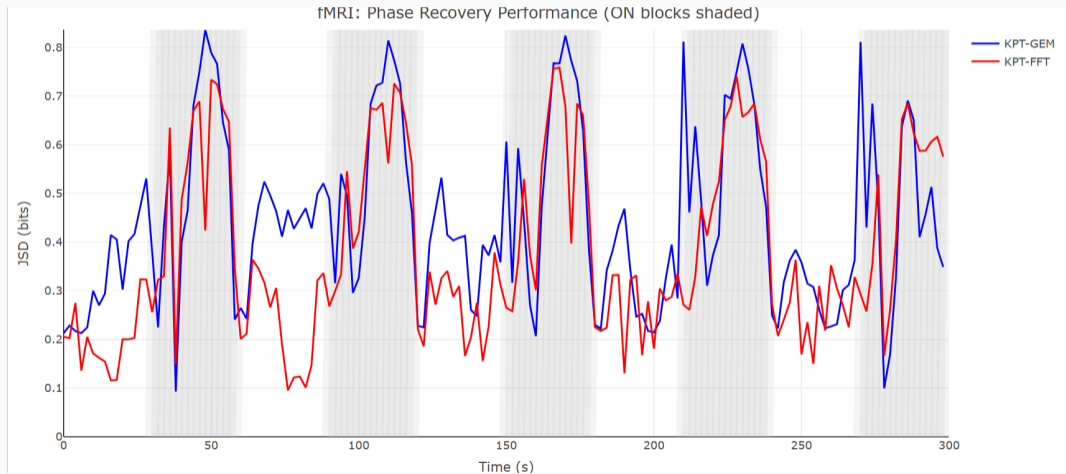


Figure: JSD (bits) across time.

# fMRI: example phase at a fixed time slice

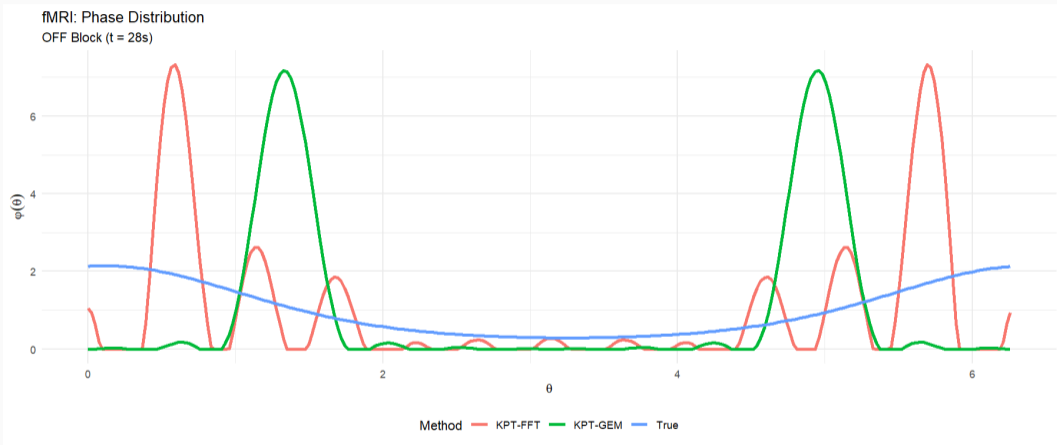
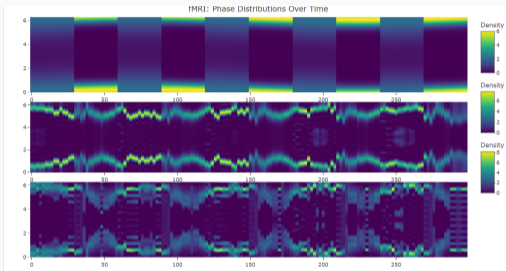


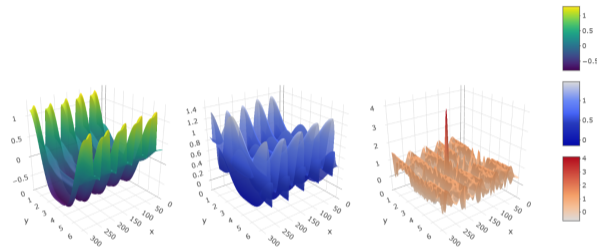
Figure: True phase  $\varphi_{t=28s}$  vs. KPT-estimated phases at the same time.

# fMRI: kime-surface heatmaps (polar) and 3D reconstructions



**Figure:** Polar heatmaps of true vs. KPT kime-surfaces.

fMRI: Kime-Surface Comparison (Aligned)



**Figure:** 3D scenes: True,  $\mathcal{S}(t, \theta)$ , and Recovered,  $\widehat{\mathcal{S}}(t, \theta)$ , kimesurfaces.

## fMRI Experiment: summary metrics

**Table:** fMRI Experiment: Summary metrics comparing true kime-surface vs. KPT reconstructions (KPT-GEM, KPT-FFT).

Algorithm	Mean JSD (bits)	Mean Hellinger	Mean TV	Rel. L2 Surface
KPT-GEM	0.4445	0.5942	0.6491	1.5013
KPT-FFT	0.3794	0.5534	0.5588	1.4574

## **5. Limitations and Opportunities**

---

## Advantages of complex-time kime-representation & KPT reconstruction

- **Beyond averaging:** explains replicate variability as structured latent state distribution  $\varphi_t$ .
- **More than warping:** phase is learned as a *distribution* (can be multimodal), not a single alignment map.
- **Beyond generic state-space:** explicit spectral deconvolution ( $M = F\Phi$ ) yields fast closed-form updates and interpretable components.
- **More than black-box deep models:** provides geometry, constraints, and inferential targets with uncertainty quantification hooks.

## KPT limitations and practical considerations

- Likelihood assumptions (e.g., Gaussian) and noise estimation can impact E-step posterior moments.
- Deconvolution ill-conditioning when  $|F(\omega, t)|$  is small (use ridge, bootstrap, or temporal coupling).
- Truncation  $J$  trades bias and variance; regularization  $(\lambda, \rho)$  must be tuned (cross-validation, predictive criteria, bootstrap).
- Directional inference requires anchoring; rotation-invariant comparisons avoid this.
- Extensions: non-Gaussian likelihoods (counts), heavy-tailed noise, anisotropic penalties in  $(t, \theta)$  aligned with  $g_0$ .

## Other Applications

- **Neuroimaging / clinical trials:** run-to-run variability decomposition; QC and stability biomarkers (space-time maps).
- **Quantum sensing / interferometry:** phase drift tomography and predictive distributions for detection patterns.
- **Coherent imaging / microscopy:** phase-aware stabilization; uncertainty-aware reconstructions.
- **Industrial IoT:** phase-state monitoring for cyclic processes and predictive maintenance.
- **Digital health:** latent physiological state distributions and personalized baselines.

## 6. Summary

---

## Key takeaways

- Kime representation augments *classical time* with a latent *phase* to account and model structured replicate variability.
- Based on replicated longitudinal process measurements and the spectral factorization  $M = F\Phi$ , KPT reconstructs

$$\left( \underbrace{\mathcal{S}(t, \theta)}_{\text{kime surface}}, \underbrace{\varphi_t(\theta)}_{\text{phase law}} \right)$$

- In practice, FFT-based Wiener-Sobolev updates provide scalable computation with principled regularization.
- *KPT outputs* enable inference (uniformity, two-sample, longitudinal), prediction, and space-kime mapping.

# Resources and reproducibility

Websites: <https://TCIU.predictive.space/> |

<https://Spacekime.org/>

Rmd-notebook: [https://socr.umich.edu/TCIU/HTMLs/TCIU\\_SK\\_Appendix03\\_KPT\\_DS\\_fMRI\\_V5.html](https://socr.umich.edu/TCIU/HTMLs/TCIU_SK_Appendix03_KPT_DS_fMRI_V5.html)

1 Introduction

2 Mathematical Framework

- 2.1 KPT Inverse Problem
- 2.2 KPT Algorithms
  - 2.2.1 Algorithm 1: KPT-GEM (Generalized EM)
  - 2.2.2 Algorithm 2: KPT-FFT (Fully Alternating)

3 Implementation

- 3.1 Core Utilities
- 3.2 Unified KPT Implementation

4 Double-Slit Experiment (with Phase Alignment)

- 4.1 Setup and Utilities
- 4.2 Double-Slit Simulation
- 4.3 Run KPT with Proper Alignment
- 4.4 Quantitative Evaluation (Post-Alignment)
- 4.5 Visualization (Aligned Results)
- 4.6 Kime-Surface Comparison

SOCR >>

TCIU Website >>

TCIU GitHub >>

Code ▾

## Time Complexity, Inferential uncertainty and Spacekime Analytics

### Appendix 03: Kime-Phase Tomography (KPT V.5: KPT-GEM & KPT-FFT): fMRI and Double-Slit Validation

SOCR Team

01/03/2026

This [TCIU Appendix](#) offers a self-contained implementation of the kime phase tomography algorithms, *KPT-GEM* (expectation maximization) and *KPT-FFT* (*FFT alternating spectral*) for estimating the phase distribution and reconstructing the kime-surface representations from observed repeated measurement data from longitudinal processes. The KPT algorithm is validated using two simulations; *double-slit physics experiment* and *fMRI ON vs. OFF neuroscience experiment*. We report quantitative performance metrics (summary tables) and provide qualitative results as surface/heatmap overlays contrasting for the *true* vs. *estimated* phase distributions and kime-surfaces.

The key steps of the KPT algorithm include E-step, Wiener-Sobolev filtering, simplex projection, and reality constraints, subject to normalization, operator conventions.

## 1 Introduction

This notebook presents a unified implementation of *Kime-Phase Tomography (KPT)*, a framework for analyzing repeated measurement longitudinal data by decomposing observations into

# Acknowledgements

- SOCR colleagues, the North Carolina State University, and the University of Michigan.
- Funding: NSF (1916425, 1734853, 1636840) and NIH (R01MH121079, R01MH126137, R41TR004515, T32GM141746, U54DE035412).
- Thank you to many SOCR collaborators, other contributors to the KPT theory, algorithms, and validation protocols, and the broader open-science community.
- Contact: [statistics@umich.edu](mailto:statistics@umich.edu).

